ANALYSING THE STRUCTURE OF WATER AT A FIXED DENSITY USING TRANSLATIONAL AND ROTATIONAL DEGREES OF FREEDOM

Dr. Jayant Balwant Patwardhan.

Associate Professor, Department of Physics, Pratap College, Amalner, Jalgaon, Maharashtra

ABSTRACT

Molecular dynamics simulations with independent thermostats for translation and rotational temperatures were used to investigate the implications of these degrees of freedom on the hydration of the ions. Our goal in this study was to determine how different charge distributions in water models affect how they react to an increase in rotational temperature. Increasing the rotational temperature, T_R, significantly breaks hydrogen bonds, according to the data. When the translational temperature, T_T, is elevated, this is not the case, at least not to this amount. With an increase in T_R, the likelihood of finding an empty spherical cavity (no water molecule present) of a given size significantly drops, although this only moderately impacts the free energy of the hydrophobe insertion at higher temperatures, a rise in T_R increases extra internal energy proportionately, but an increase in T_T has a considerably lesser effect.

Keywords: Water models, Degrees of freedom, Magnitude, Hydrogen, Molecules

I. INTRODUCTION

Most of water's characteristics have been measured with excellent precision at air or moderate pressure, making it the most well-known material in nature. HP water has also been the focus of various research because of its impact on a wide range of sciences, from condensed matter physics to planetology. Water's structural and vibrational characteristics have been studied up to several GPa, but the knowledge of water self-dynamics under high pressure is still lacking. Water diffusion under high pressure (HP) settings is critical to a wide range of practical and basic scientific questions. Intermediate-depth seismicity is strongly influenced by the diffusion of water at pressures of a few GPa, which occurs in the transition zone of the Earth's mantle. Computer simulations at pressures of several GPa anticipate the emergence of new phases of water with distinctive diffusive behaviour, such as the free rotation of water molecules (plastic phases) or proton free diffusion (superionic phase). For accurate simulations of planet interiors, it is critical that they be well characterized.

In addition to solute-solute interactions, solutions' properties are also influenced by the solvent's capacity to solvate the solute particles. Polyelectrolytes and proteins, which have hydrophobic and ionic groups, are important in electrochemistry, geochemistry, and biology.

A number of intriguing issues have been raised recently about the significance of basic degrees of freedom in hydration (translation, rotation, and vibration). Interaction of microwaves with aqueous solutions can lead to a meaningful physical condition, which has been examined using non-equilibrium molecular dynamics simulations with an explicit electric field represented. The steady state molecular dynamics simulations with independent thermostats for different degrees of freedom were studied by Bren and Jane. Hydration of hydrophobes and cations was studied in the presence of varied rotational and translational temperatures.

II. MODEL AND SIMULATIONS

Molecular dynamics simulations were run using 256 SPC/E water molecules in the simulation box at a fixed number of particles and volume (N, V). There were no changes made to the numerical density of water molecules 1.0 g/cm^3 or the time step employed in this

experiment, which were both set at 1.0 fs. For each MD simulation, an MD equilibration run of at least 100 ps in length was performed, and data were gathered during a production run of 4900 ps.

Translational motion of a molecule was characterized by its center-of-mass location r_i, its velocity v_i and the force f_i acting on it. Similarly, the rotational motion of a single water molecule i was defined by its orientation (using the quaternion representation) q_i, angular velocity I and torque i. While the acceleration of the mass centre is directly proportional to the force applied on it, the angular acceleration must be calculated using Euler's equations of motion for rigid bodies. sTo integrate the equations of motion, we used the well-known Verlet technique. We used a basic velocity rescaling approach to keep T_R and T_T constant at their original values.

III. RESULTS AND DISCUSSION

3.1 Radial distribution functions

The oxygen–oxygen and oxygen–hydrogen distribution functions, g_{OO} and g_{OH}, are the first to be shown numerically. On the left, we show the g_{OO} distributions for various rotational (T_R) and translational temperature values.

There are two ways that temperature affects an oxygen–oxygen distribution function's initial peak. In terms of how the peak's location changes with temperature, there is a distinction. As T_R rises, the first peak moves outwards into greater distances. Conversely, a rise in translational temperature, T_T does not alter the position of g_{OO}'s initial peak. There is a noticeable increase in the peak's width; this suggests that molecules with more kinetic energy may more easily "penetrate" into one other.

The second peak in this graph depicts ambient conditions for liquid water (figure 1). As hydrogen bonds are absent, the peak is at 4.5 Å rather than 2σW W ~ 6 Å. The water molecules' hydrogen bonds account for this peak's location. The shift of the second peak toward ~ 6 Å shows that some hydrogen bonds break following an increase of rotational temperature. Figure 2 depicts the model water's hydrogen bonds as they are affected by temperature changes. g_{OH}, the oxygen-to-hydrogen ratio, is shown against temperature in this figure.

It is important to note the location of the first peak in the graphite oxide distribution (g_{OH}). We can observe that the height of this peak is quite sensitive to T_R fluctuations, whereas the T_T variations have a considerably less effect on the peak's height. Although the peak is less in both situations, it is still significant. The coordination number, n_H, is derived from this distribution (for the definition see caption in figure 3). Figure 3 show that T_R has a roughly linear effect on this number. At higher temperatures, n_H, on the other hand, is substantially less sensitive to changes in T_T.

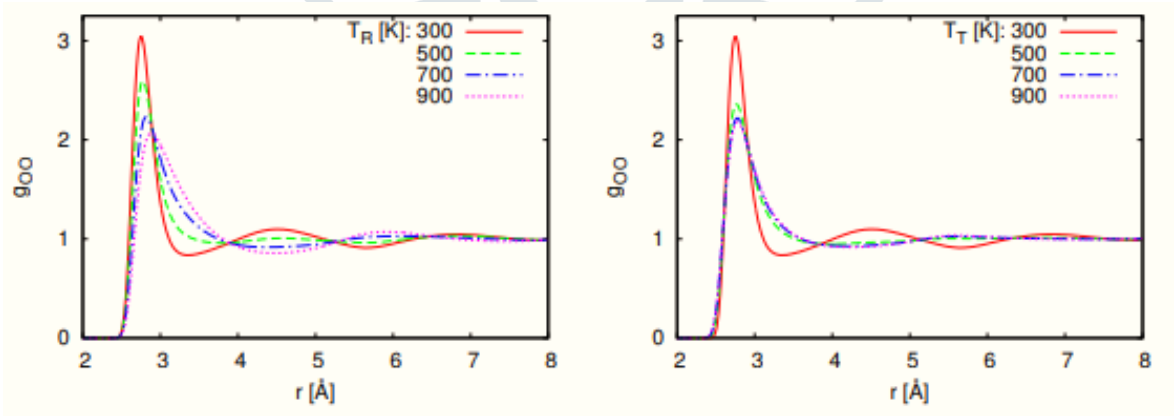

Figure 1: (Color online) Oxygen–oxygen radial distribution functions (gOO) for different TR (left-hand) and TT (right-hand) values. Different lines correspond to different values of the relevant temperature: 300 K (solid, red), 500 K (dashed, green), 700 K (dash-dotted blue), and 900 K (dotted, magenta).

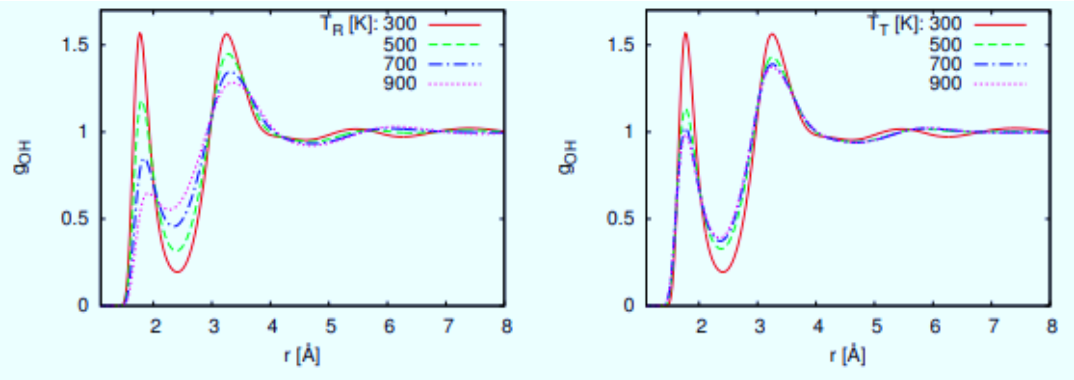

Figure 2: (Color online) Oxygen–hydrogen radial distribution functions (g_{OH}) for different T_R (left-hand) and T_T (right-right) values. The color code as for figure 1

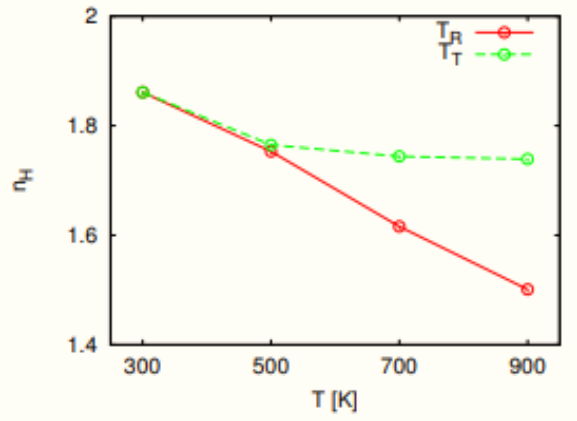

Figure 3: (Color online) Coordination number, n_H, of hydrogen atoms of the neighbouring molecules around oxygen of the central molecule (and vice versa) as a function of T_R (solid, red) and T_T (dashed, green). n_H is obtained as the volume integral of g_{OH} up to the first minimum (at 2.4 Å).

Water molecules can form N_{HB} hydrogen bonds with a probability $P(N_{HB})$ seen in Figure 4. The probability distribution, $P(N_{HB})$, for T_R and T_T dependency is nearly identical up to 500K. Above T_R=500 K, the apex of this distribution is gradually moved toward lower N_{HB} values and there is a considerable likelihood for only one hydrogen bond. The scenario is different with an increase of T_T where the $P(N_{HB})$ distribution does not alter substantially upon an increase of the translational temperature above T_T=500 K.

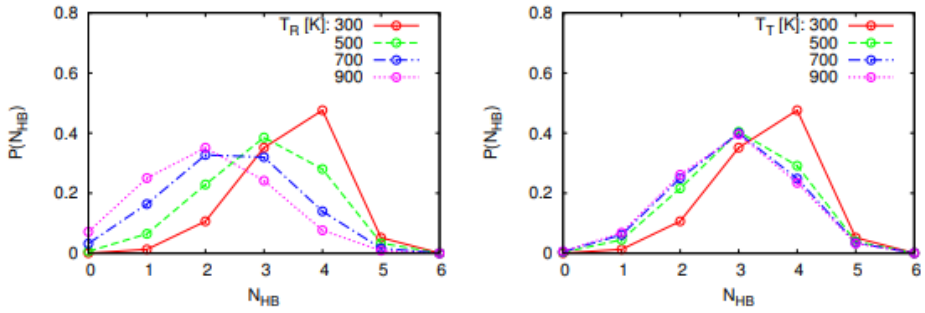

Figure 4: (Color online) Probability for a water molecule to form N_{HB} hydrogen bonds, $P(N_{HB})$, at different T_R (left-hand panel) and T_T (right-hand panel). We count two water molecules as hydrogen-bonded if (i) the angle between the OH arm of one molecule and the O–O vector is less than 30◦ , and (ii) if the O–O distance is less than 3.3 Å (position of the first minimum in g_{OO}). The color code as for figure 1

So far, all the data points to hydrogen-bonding being more susceptible to TR alterations than TT variants. The development of a hydrogen bond necessitates the proper alignment and spacing between two water molecules. It is easy to realize that any increase in TR (faster rotation) will make advantageous orientations less probable. At situations of high TR, the model molecules will operate as independent rotators with the hydrogen bond interaction energy approaching zero.

When the T_T rises, the mechanism that causes two water molecules to lose their correlation changes. However, because each molecule is encased by the others, this is not a simple task because they must be separated by a particular distance. Even at high temperatures (T_T=900 K), the system is subject to the strong repulsive contact that results from rising TT while simulating at a constant water density. With a rise in T_T (to T_T = 500 K), the radial order is disturbed and some hydrogen bonds are broken.

If the radial distribution function, g_{OO}, is separated into the independent contributions of the nearby molecules coordinated on the selected molecule, further information about the water structure can be acquired. In our notation, g_i is the contribution of the i-th neighbor to the overall pair distribution function. On the left, the findings are displayed in figure 5, while on the right; the results are shown at different translational and rotational temperatures. When TR increases, we see the peaks moving outwards to greater distances. This applies to all four nearest neighbors. At this density water molecules are densely packed; whereas σWW for this (SPC/E) model is 3.169 Å, the location of the first peak is really at roughly 2.7 Å. The molecules are dispersed over greater average distances as a result of an increase in T_R. In contrast to this, an increase in the T_T does not appreciably modify the position of the first peak. This is another consequence of the fact that quicker rotation (increase in T_R) disturbs the hydrogen bond network more efficiently than an increase in T_T.

An anonymous reviewer has presented an intriguing topic about the differences in peak locations of various g_i's when the TR is increased. First peak, g_1, appears to be less influenced than more distant peaks, such as g_3 and G_4 in Figure 5. Why? Given that g_3 measures the oxygen–oxygen distribution function's third neighbor's contribution, we may infer that the central molecule's connection with the third shell molecules is greatly reduced.

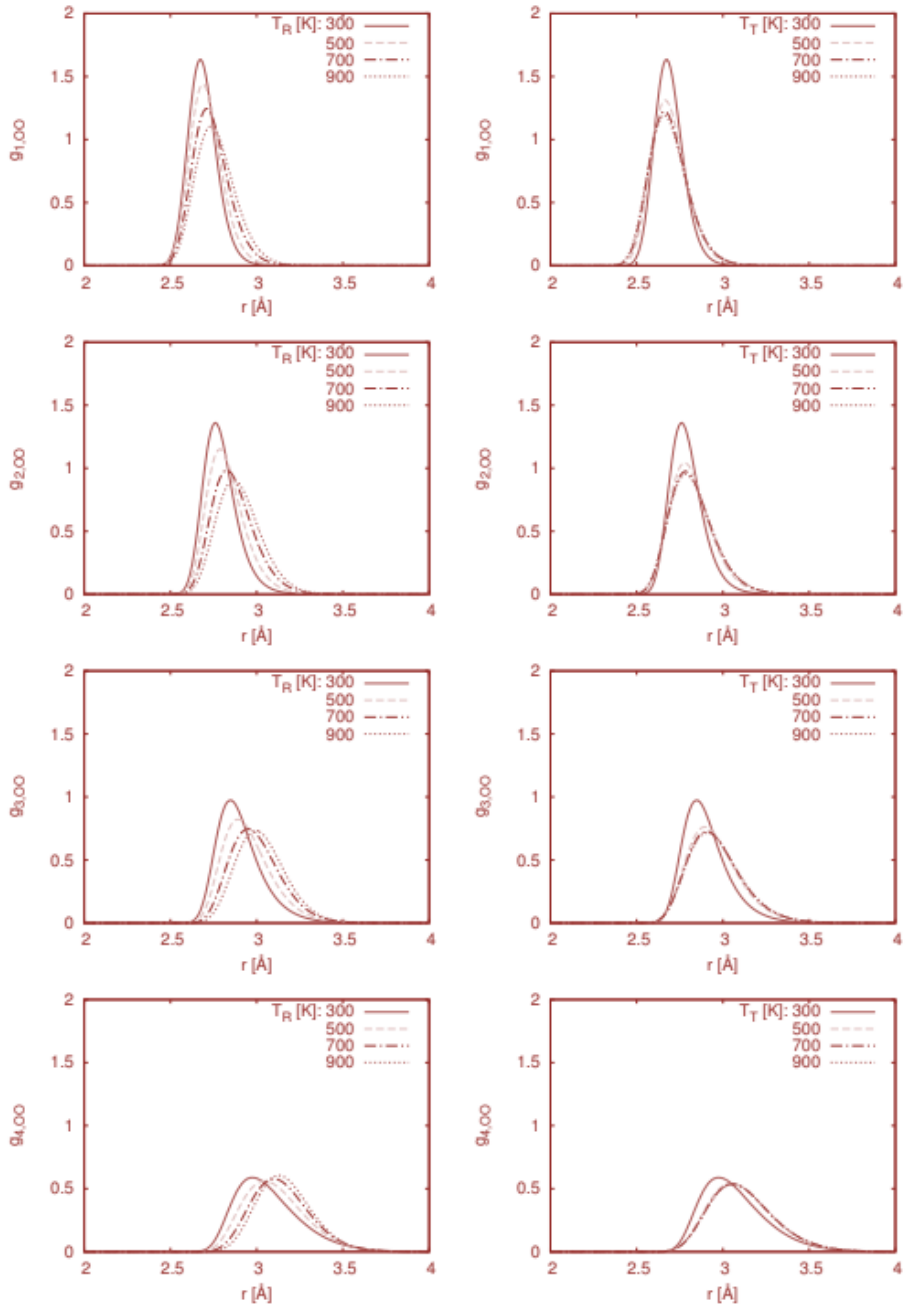

Figure 5: (Color online) Oxygen–oxygen radial distribution function for the first four neighbours of the water molecule (from top to the bottom g_1 to g_4) at different T_R (left-hand panels) and T_T (right-hand panels). The color code as for figure 1

To put it another way, the core molecule's impact on the bulk does not extend that far. Figure 1 show that increasing T_R or T_T leads to a more uniform distribution of oxygen–oxygen pairs in the solution, which is quantified by the g_{OO} distribution function. In addition, when the temperature rises, the oscillations become "out of phase."

3.2 Probability of observing an empty cavity of a size of water

Using a fixed number of particles in a fixed volume, the simulations provided in this work are accurate. The density variations in a liquid system provide valuable information. A probability distribution P(N) for finding exactly N water molecules (really their centers of gravity) in a 3 diameter circular volume was examined in this subsection, and the results are presented in the following table: For tiny volumes (molecular size), the probability distribution is almost Gaussian. In terms of compressibility, a broader distribution indicates a larger degree of compressibility. As T_R and T_T rise, our simulations show that the P(N) curves only slightly alter. However, the chance of finding an empty spherical hollow (P (0)) is one significant exception. In this way, just P ($0T_R$)'s and T_T dependences are presented in figure 6. With a T_R rise from 300K to 900K, P (0) is reduced by nearly an order of magnitude (note the natural logarithm plotted on y-axis in figure 6). A reduction in hydrogen bonding reduces density

fluctuations. In contrast, there is little impact on P from changes in T_T (0).

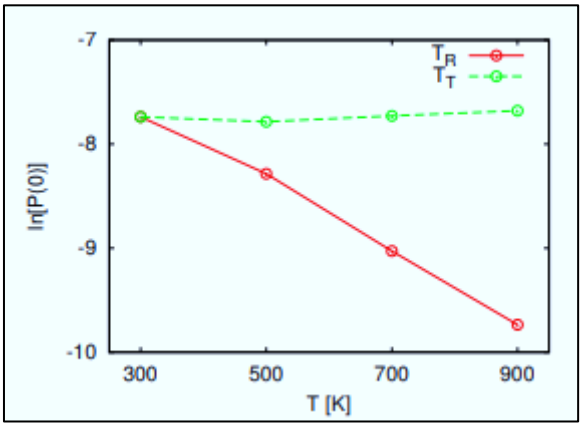

Figure 6: (Color online) Logarithm of probability P(0) of observing an empty spherical cavity of diameter 3 Å in the model water as a function of T_R (solid, red) and T_T (dashed, green).

The thermodynamic integration of a hydrophobe insertion, ΔFins, into the model water was also done as a supplement to these results (see figure 7). The Lennard-Jones particle, with a well depth equal to that of the model water molecule and σSS = 3, was used to simulate the hydrophobe. In the case of cross-interaction parameters, the Lorentz-Berthelot mixing rule was employed. The hard-sphere solute should have the same amount of Fins as the hydrophobe under weak hydrophobe–water coupling circumstances.

When T_R is increased, P (0) values fall, but insertion free energy is only marginally influenced. Although T_T has little effect on the P (N) distribution, it has a significant impact on the Fins. Adding a hydrophobe to the system becomes more difficult as the free energy required inserting the particle, Fins, rises in both circumstances.

In this section, we attempt to provide a more in-depth explanation for this finding. Hard-sphere solute insertion free energy is proportional to the likelihood of finding an empty spherical cavity in the solvent, P (0). (As usual k_B is the Boltzmann constant):

$$\Delta F_{\text{ins}} = -k_B T \ln P(0). \qquad \textbf{(1)}$$

Equation (1) refers to the translational temperature because the solute–water interaction is only dependent on the positions (and not the orientations) of water molecules and since equation (1) applies to any solvent (not necessarily containing rotational degrees of freedom). P(0) values fluctuate greatly with T_R, while the lnP(0) only rises in magnitude by around 20%, which is near to the relative change of ΔFins with T_R. The increase in Fins can be explained to an increase in the pre-factor K_{BT} when T_T rises.

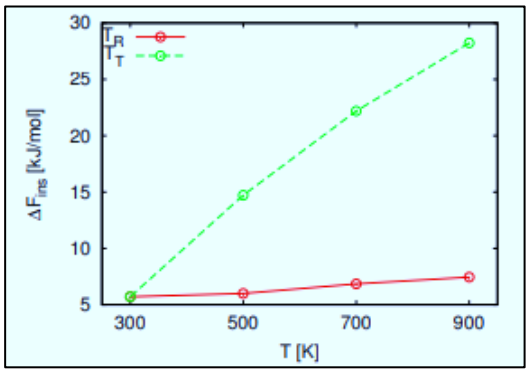

Figure 7: (Color online) Free energy of the hydrophobe insertion as a function of T_R (solid, red) or T_T (dashed, green).

3.3 Excess internal energy

Studying changes in E_{ex} per mol of water molecules as a function of T_R or T= is an interesting exercise (figure 8). We can observe that as T_R increases, E_{ex} increases virtually linearly, but when T_T increases, the same amount changes less and less. As previously stated, this behavior is due to the differing effects of hydrogen bonding's two degrees of freedom. T_R and T_T influences on the surplus heat capacity (at constant N/V) $C_{v,r}^{ex}$ *and* $C_{v,t}^{ex}$ may be seen in these graphs. It's clear from this graph that rotational heat capacity (the derivative of the top curve) is temperature independent, but translational heat capacity (the derivative of the bottom curve) drops to zero at very high temperatures.

3.4 Dynamics of model water molecule upon an increase of T_R and T_T

What effect do the various degrees of freedom have on water molecule dynamics? Figure 9 shows the influence of T_R and T_T on a model water molecule's (self) diffusion coefficient.

Hydrogen bonds are broken as a result of a rise in T_R, resulting in quicker diffusion. It is easier for water molecules to disperse since they are less tightly connected together. However, a rise in TR results in a fall in P (0). A random walk should thus take smaller steps, which will slow down the diffusion. At the greatest TR tested here, this impact appears to predominate. T_T, on the other hand, increases the diffusion coefficient monotonically in this temperature range.

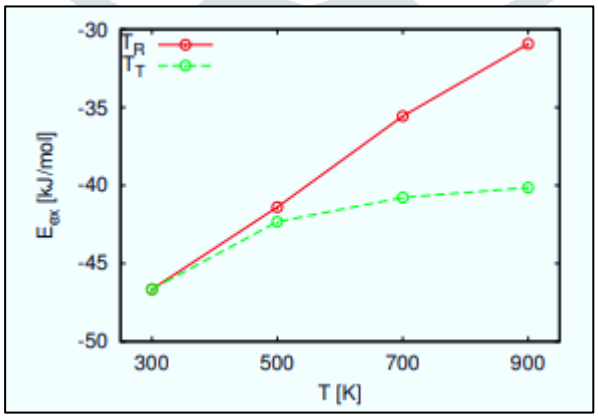

Figure 8: (Color online) The excess internal energy per mol (E_{ex}) as a function of T_R (solid, red) and T_T (dashed, green).

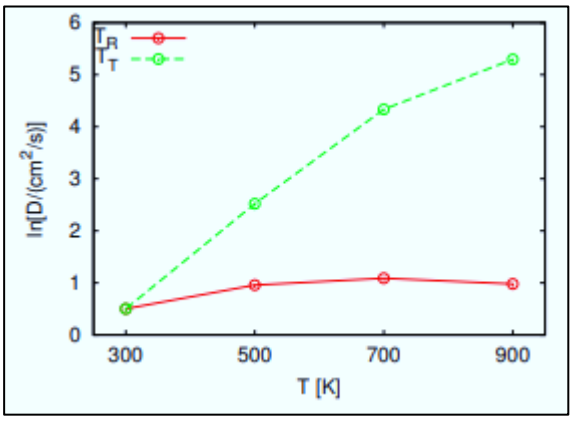

Figure 9: (Color online) Diffusion coefficient as a function of T_R (solid, red) or T_T (dashed, green). Note the logarithmic scale on y-axis.

IV. CONCLUSIONS

It is generally known that microwaves generate heating through excitation of rotational motion in water molecules and that the rotational kinetic energy is subsequently transferred to the translational degrees of freedom. The microwave irradiation is crucial in biology: there are claims that microwaves improve the folding and unfolding dynamics of globular proteins, as well as protein aggregation.

The influence of microwaves on the characteristics of liquids and solutions may be examined via non-equilibrium molecular dynamics simulations. In such investigations, the electric field is simulated explicitly. Following the principles, we undertake computations in which the rotational degree of freedom has the temperature distinct from the translational one. We explored the influence of such non-equilibrium situations on the solvation of simple solutes. In the current contribution, we explored the characteristics of model water under non-equilibrium settings where the translational and rotational temperatures fluctuate separately. An rise in the rotational temperature leads the first peak of g_{OO} to migrate toward bigger distances, whereas its location stays unaltered upon T_T increase. The height of the initial peak in the hydrogen–oxygen distribution function is substantially more dependent on the T= than on the T_T changes. At high rotational temperatures, the number of hydrogen bonds may drop as low as to one. Free energy of the hydrophobe insertion does only minimally rely on the rotating temperature. Water diffusion coefficient assessed using the mean square displacement is, in contrast to the T_T dependency, a non-monotonous function of the rotational temperature. These and other effects seen upon modifying the rotational temperature may dramatically influence the characteristics of water as solvent, which has to a considerable degree been explored. The study examining such effects on polymer and polyelectrolyte conformations in aqueous solution is now underway — preliminary results clearly suggest toward a significant possibility of polymer collapse in circumstances of rotational heating.

REFERENCES: -

1. Mohorič, Tomaž & Hribar-Lee, Barbara & Vlachy, Vojko. (2014). Effects of the translational and rotational degrees of freedom on the hydration of simple solutes. The Journal of chemical physics. 140. 184510. 10.1063/1.4875280.

2. Konyukhov, Vadim. (2014). The Water Molecule with Conjoint Translational, Rotational and Spin Degrees of Freedom in the Gas and Liquid Phases. Universal Journal of Physics and Application 2(6): 302-309, 2014. 2. 302-309. 10.13189/ujpa.2014.020604.

3. Y. Shan, et al., Nature Structural & Molecular Biology 2014, 21, 579–584. http://dx.doi.org/10.1038/nsmb.2849

4. Bove, Livia & Klotz, S & Strässle, Th & Koza, Michael & Teixeira, José & Saitta, Antonino. (2013). Translational and Rotational Diffusion in Water in the Gigapascal Range. Physical review letters. 111. 185901. 10.1103/PhysRevLett.111.185901.

5. S. Klotz, in Techniques in High Pressure Neutron Scattering, (CRC press, Boca Raton, 2012).

6. A. Ben-Naim, in: Molecular Theory of Water and Aqueous Solutions. Part I: Understanding Water, World Scientific Publishing Co. Pte. Ltd., Singapore, 2010, pp. 280–564.

7. Mazza, Marco G. & Giovambattista, Nicolas & Stanley, H. & Starr, Francis. (2007). Connection of translational and rotational dynamical heterogeneities with the breakdown of the Stokes-Einstein and Stokes-Einstein-Debye relations in water. Physical review. E, Statistical, nonlinear, and soft matter physics. 76. 031203. 10.1103/PhysRevE.76.031203.

8. Mazza, Marco G. & Giovambattista, Nicolas & Starr, Francis & Stanley, H.. (2006). Relation between Rotational and Translational Dynamic Heterogeneities in Water. Physical review letters. 96. 057803. 10.1103/PhysRevLett.96.057803.